

Supporting Online Material

Supplementary Materials and Methods

Supplemental Text

Supplemental Figures

Table

Supplemental References

Supplementary Materials and Methods

Rat lung harvest. Lungs were harvested from young adult (3 month-old) male Fischer 344 rats (Charles River, Wilmington, MA). All animal experimental work was performed with approval from the Yale University Institutional Animal Care and Use Committee. All animal care complied with the Guide for the Care and Use of Laboratory Animals. Animals were euthanized via intraperitoneal injection of sodium pentobarbital (Sigma, 140 mg/kg) and heparin (250U/kg). Immediately after euthanasia, the abdomen was entered via a transverse incision just below the costal margin. The diaphragm was punctured, and the rib cage was cut to reveal the lungs. The lungs were perfused via the right ventricle with PBS containing 50 U/ml heparin (Sigma) and 1 µg/ml sodium nitroprusside (SNP, Fluka). After perfusion was complete, the heart, lungs and trachea were dissected free and removed en bloc. Tracheal and pulmonary artery cannulae were inserted, with the arterial cannula entering via the right ventricle of the heart.

Lung epithelial cell isolation and culture. Lung epithelial cells were isolated from neonatal (<7 day-old) Fischer 344 rats in accordance with the Yale University Institutional Animal Care and Use Committee. Isolated lungs were rinsed in Dulbecco's modified Eagle's medium (DMEM, Gibco) and minced into fine tissues. Tissues were digested with elastase for 20 minutes (4U/ml in DMEM with 100U/ml DNase) followed by a 1 hour digestion with collagenase (1mg/ml in 1:1 DMEM:PBS with Ca²⁺ and Mg²⁺). Digested tissues were filtered through a 70 µm filter and rinsed with DMEM several times. Epithelial cells were cultured in DMEM with 10% FBS and antibiotics.

Rat lung microvascular endothelial (RMECs) were purchased from VEC Technologies (Rensselaer, NY). Cells were cultured on 1 µg/cm² fibronectin-coated (Gibco) polystyrene tissue culture flasks in MCDB-131 "complete medium" (VEC Technologies) supplemented with 10% FBS, antibiotics and growth factors. Fresh culture medium was exchanged every 3-4 days. RMECs were passaged when they reached 80% confluency using 0.25% trypsin-EDTA (Gibco) and used between passage 3 and 5.

Bioreactor design and components. All bioreactor components were obtained from Cole-Parmer (Vernon Hills, IL). A silicone stopper and 500ml glass jar formed the basis of the bioreactor. PharMed tubing (Westlake, OH), sizes L/S 14 and L/S 16, was inserted through the silicone stopper to enable the necessary connections to the lung, including a perfusion loop and ventilation with either medium or air. Pressure was monitored using a TruWave pressure transducer (Edwards Lifesciences, Irvine, CA) between the perfusion pump and the connection to the pulmonary artery. Perfusion was accomplished using a Masterflex L/S variable speed roller pump (Masterflex, Vernon Hills, IL), with perfusion rates of 1-5ml/min. Ventilation was performed using a multichannel programmable syringe pump (Cole Parmer) at 1 breath/min.

A diagram and schematic of the bioreactor is shown in Figure 1. For decellularization, a simplified version of this bioreactor was utilized.

Rat lung decellularization. Freshly harvested lung tissue was transferred to a bioreactor and kept at 37°C. The pulmonary arterial pressure was monitored throughout the decellularization process and kept below 20mmHg. Decellularization was performed using 8mM CHAPS, 1M NaCl, and 25mM EDTA in PBS (1). Lungs were inflated with decellularization fluid and perfused with PBS for 30 minutes, after which decellularization fluid was perfused through the vasculature for an additional 2-3 hours, until 500ml of fluid had perfused the lung. After decellularization, lungs were rinsed extensively with PBS and sterilized with 10% penicillin/streptomycin (Gibco). Lungs were treated with benzonase (90U/ml, Sigma) and rinsed in PBS containing 10% FBS to remove remnant DNA (2).

Rat lung recellularization. Prepared scaffolds were rinsed in culture medium and transferred to a tissue culture incubator for culture at 37°C and 5% CO₂. Neonatal epithelial cells were seeded into the airway compartment as a concentrated cell suspension of ~10 million cells/ml. Epithelial cells were seeded immediately after isolation, without a preplating step. Each lung received typically 100 million epithelial cells, and was fully inflated with the cell suspension. After static overnight culture to enable cell adherence, lungs were perfused through the vasculature at 1-5 mL/min or ventilated through the airways via negative pressure at 1 breath/min. Lung microvascular endothelial cells were seeded via injection into the vasculature at 3 mL/min, with each lung receiving approximately 30 million endothelial cells. To enable diffuse endothelial cell seeding, the scaffolds were ventilated during administration of the endothelial cell population. During epithelial culture, lungs were grown in DMEM with 10% FBS and antibiotics. During endothelial culture or co-culture of both cell types, engineered tissues were grown in MCDB-131 complete medium. Culture periods generally varied from 4-8 days. For implantation of engineered lungs, acellular matrices were re-populated with neonatal rat lung epithelium for 3-5 days, under conditions of negative pressure liquid breathing in the presence of DMEM with 10% FBS. Then, lung microvascular endothelium was seeded into the vasculature, culture medium was switched to MCDB-131 complete medium to support endothelial growth and survival, and culture continued for 24-36 more hours.

Orthotopic lung transplantation. Syngeneic male, 3-month old Fischer 344 rats were used as recipient animals for orthotopic lung transplantation. Experiments were performed in accordance with the Yale University Institutional Animal Care and Use Committee. Recipient animals were anesthetized, intubated and ventilated with 100% O₂. Anesthesia was maintained with inhaled isoflurane and animals were anticoagulated with heparin (100U/kg). Left lung transplantation was performed following standard rodent surgical techniques (3). Briefly, a left thoracotomy was performed, and the left hilum was dissected to expose the left pulmonary artery, vein and bronchus. The recipient native left lung was ligated and removed. A left engineered lung was dissected and the left pulmonary artery, vein and bronchus were anastomosed to the recipient using 10-0 suture. The bronchus of the engineered lung was unclamped and the lung was ventilated with 100% oxygen without perfusion for 5 minutes, after which the pulmonary artery and vein were unclamped to initiate blood flow to the engineered lung. Gas exchange in the engineered lung was assessed via blood gas analysis of the left pulmonary artery and vein. To ensure that pulmonary venous samples were not contaminated by cross-flow

from the native right lung, the left pulmonary vein was temporarily clamped with a surgical clip before drawing venous samples from the engineered lung. Blood gas values were assessed using an i-STAT portable clinical analyzer (i-STAT, East Windsor, NJ).

The engineered lungs were implanted for up to 2 hours, after which the recipient animals were euthanized and the implanted lungs harvested.

Histological analysis and immunofluorescence. For histological evaluation of the decellularized and engineered lung tissue, samples were fixed in 10% formalin for 4 hours, dehydrated, embedded in paraffin, and sectioned at 5 μm . Sections were stained with hematoxylin and eosin stain (H&E), as well as 4',6-diamidino-2-phenylindole (DAPI) for DNA.

For immunofluorescence, tissue sections were deparaffinized, rehydrated, and rinsed in PBS with 0.2% Triton X-100 for 15 minutes. Antigen retrieval was performed with 0.01M citric acid, pH 6.0, at 70°C for 20 minutes. Sections were then blocked with 5% BSA and 0.75% glycine in PBS for 1 hour at room temperature. Primary antibodies were applied at the concentrations given in Table S1 in blocking buffer overnight at 4°C, followed by secondary antibodies at 1:500 dilution for 1 hour at room temperature. Secondary antibodies used were AlexaFluor 555 donkey anti-goat or goat anti-rabbit and AlexaFluor 488 chicken anti-rabbit (Invitrogen). Slides were mounted using DAPI-containing mounting media (Vector Labs), and images acquired using a Zeiss Axiovert 200M inverted fluorescent microscope.

DNA assay. DNA content of tissues was quantified using the Quant-iT PicoGreen dsDNA assay kit (Invitrogen, Eugene, OR), following manufacturer's instructions. Briefly, tissue samples were weighed and lyophilized, diluted in TE buffer and mixed with the Quant-iT PicoGreen reagent. Fluorescence was measured at 535nm with excitation at 485nm, and DNA content was quantified using a standard curve.

Collagen assay. Collagen was quantified with a colorimetric assay to detect hydroxyproline (4). Briefly, papain-digested samples were incubated in 6 N HCl at 115°C for 18 hours, neutralized, oxidized with chloramine-T and reacted with p-dimethylaminobenzaldehyde (Mallinckrodt Baker, Phillipsburg, NJ). Absorbance was measured at a wavelength of 550 nm and a 1:10 w/w ratio of hydroxyproline to collagen was used to calculate the collagen content of the tissue.

Elastin assay. Elastin was quantified using the Fastin Elastin assay kit (Biocolor, Belfast, N. Ireland). Lung samples were first lyophilized and weighed, and then the elastin was extracted following described methods (5). Samples were incubated with 0.25M oxalic acid at 100°C, then centrifuged at 10,000g and the supernatant saved. The supernatant from 5 extractions was pooled, and the supernatant from the 6th extraction was also measured to ensure that no more elastin remained in the tissue. The oxalic acid was cleared using a 10,000 molecular weight cutoff filter (Millipore), then resuspended in dH₂O and analyzed using the Fastin Elastin kit according to the manufacturer's instructions.

Sulfated glycosaminoglycan (GAG) assay. Sulfated glycosaminoglycans, including chondroitin, dermatan, heparan and keratan sulfates, were quantified using the Blyscan GAG assay kit. Papain-digested samples were assayed according to the manufacturer's instructions. Briefly, sulfated GAGs were labeled with 1,9-dimethyl-methylene blue dye and absorbance was measured at 650 nm.

Western Blotting. Tissues were digested in RIPA buffer (50mM Tris-HCl, pH 7.4, 150mM NaCl, 1% [v/v] Triton X-100, 0.5% [w/v] sodium deoxycholate, and 0.1% [w/v] SDS, Boston Bioproducts) with freshly added protease inhibitors (Sigma) and homogenized at 15,000 rpm for 30 seconds. After incubation for 1 hour at 4°C, insoluble particles were removed by centrifugation at 14,000g for 25 minutes. Protein concentration was quantified via Bradford assay, then boiled in Laemmli's reducing buffer (Boston Bioproducts) for 25 minutes at 65°C. Protein was electrophoresed on polyacrylamide gels, transferred to a nitrocellulose membrane, and blocked for 1 hour in 5% non-fat dry milk (NFDM) or 3% bovine serum albumin (BSA) in TBS with 0.05% tween-20 (TBS-T). Primary antibodies were applied overnight in 2% NFDM or 3% BSA in TBS-T, followed by horseradish peroxidase-conjugated goat or donkey secondary antibodies (Santa Cruz) for 1 hour at room temperature at a dilution of 1:2000. Antibody source and dilutions are given in Table S1. Protein was detected using substrate from Supersignal West Pico.

Scanning electron microscopy (SEM). Samples were fixed using 2% glutaraldehyde and 2.5% paraformaldehyde in 0.1M cacodylate buffer (EMD Biosciences, Gibbstown, NJ) for 2 hours at room temperature, then rinsed in cacodylate buffer, sliced, and dehydrated through an ethanol gradient. Samples were further dehydrated in hexamethyldisilazane for 10 minutes and dried overnight, then sputter coated with gold and analyzed using a JOEL JXA-8600.

Transmission electron microscopy (TEM). Samples were fixed using 4% paraformaldehyde in PBS and then placed in 2% glutaraldehyde and 2.5% paraformaldehyde in 0.1M sodium cacodylate buffered fixative for 2 hours at room temperature. The samples were rinsed in 0.1M sodium cacodylate buffer and postfixed in 1% osmium tetroxide for 1 hour, then en bloc stained in 2% uranyl acetate in maleate buffer pH 5.2 for a further hour. Then, the samples were rinsed, dehydrated through a graded ethanol series and infiltrated with epon resin and baked overnight at 60°C. Hardened blocks were cut using a Leica UltraCut UCT and 60 nm sections were collected on nickel grids and stained using 2% uranyl acetate and lead citrate. Samples were viewed on a FEI Tencai Biotwin TEM at 80kV. Images were taken using a Morada CCD digital camera using iTEM (Olympus) software.

Micro CT imaging. Native or decellularized lungs were fixed in 10% neutral buffered formalin and injected with contrast agent through either the airway or vasculature. Contrast agent was 20% bismuth and 5% gelatin in PBS. After injection of contrast, the lung was cooled in an ice bath to polymerize the gelatin.

Prepared lungs were imaged with a micro-CT imaging system (GE eXplore Locus SP, GE Healthcare), set to a 29 μm effective detector pixel size. The micro-CT was operated at 60kV peak x-ray tube voltage, 80 mA tube current, 1600 millisecond per frame, 22 detector binning model, 720 views, and 0.5° increments per view. For the high resolution imaging of one lobe (right superior lobe), samples were positioned on a computer-controlled rotation stage and scanned 360° around the vertical axis in rotation steps of 0.4°. The tube is operated at an 80 kV peak and 80 mA. The exposure time for each view was typically 3000 millisecond, with detector binning model set to 1x1 and resolution of 6.5 μm . Both acquisitions resulted in a set of contiguous axial VFF-formatted images through the lung or one lobe.

With the use of Microview Software (GE Healthcare), the raw data was corrected and reconstructed with voxels of dimensions $58\ \mu\text{m} \times 58\ \mu\text{m} \times 58\ \mu\text{m}$ to visualize the whole vascular tree in the lung. For the high-quality image of the vascular tree (one lobe), voxels were set to $6.5\ \mu\text{m} \times 6.5\ \mu\text{m} \times 6.5\ \mu\text{m}$. This software was also used to reconstruct maximum intensity projection images from the raw data. Multiplanar reformation, spatial filtering, and volume rendering techniques allowed us to view the data set in transverse, sagittal, coronal, hybrid planes, and 3D format. Binarized images were used for object extraction and region-of-interest measurements. Three-dimensional volume images are reconstructed from the angular views by using a modified Feldkamp filtered back-projection algorithm.

Mechanical stress-strain testing. Native, decellularized and engineered lung samples were analyzed using an Instron 5848 equipped with a 10N load cell. Slices of tissue of known dimensions were cyclically pre-stretched for 10 cycles to 20% strain to investigate elastic properties and then stretched until failure to evaluate ultimate tensile strength (UTS). Using tissue dimensions, engineering stress and strain were calculated from force and distance.

Compliance testing. Native, decellularized and engineered lung tissues were inflated with air using a syringe pump (Cole Parmer, Vernon Hills, IL) and the tracheal pressure was monitored using a TruWave pressure transducer (Edwards Lifesciences, Irvine, CA). Lungs were inflated to full inflation (corresponding to $\sim 10\text{ml/kg}$ of original animal weight) under quasi-static conditions. Compliance values on the upstroke of the inflation curve were calculated from the slope of the curve, expressed in mL/mm Hg.

Decellularization of human lung. A human lung from an anonymous donor was obtained from a tissue repository (Integrated Laboratory Services – Biotech) and utilized in accordance with the policies of the Yale University Human Research Protection Program. The bronchus and pulmonary artery of the left upper lobe were cannulated and the lung was flushed with saline through the vasculature. The lung was perfused with decellularization fluid for 6 hours at room temperature, with perfusion pressure maintained under 25 mmHg. Following extensive rinsing with PBS, the lung was cut into thin (1-2mm) slices and sterilized using 10% penicillin-streptomycin and 4% amphotericin-B (Gibco).

Recellularization of human lung. Human endothelial progenitor cell-derived endothelial cells were obtained from discarded cord blood samples by isolation following established protocols and in accordance with the Yale University Human Investigation Committee (6). Endothelial cells were propagated in endothelial growth medium 2 (EGM-2, Lonza) and used at passage 4. Human carcinoma alveolar basal epithelial cells, A549, were cultured in F-12K medium (American Type Culture Collection, Manassas, VA) supplemented with 10% FBS (Thermo Scientific) and used at passage 83. After a 30-minute incubation with 1 mL of a 1×10^6 cells/mL cell suspension (containing endothelial cells, epithelial cells, or both), slices of cell-seeded human lung matrix were cultured for 4 days in a multi-well tissue culture plate (Becton Dickinson). Acellular matrices repopulated with endothelial cells were cultured in EGM-2 and matrices repopulated with A549 epithelial cells were cultured in F12K with 10% FBS. Matrices seeded with a combination of cells were also cultured in EGM-2, and medium was changed every day.

Supplemental Text

Bioreactor design features. The lung bioreactor contains a main reservoir wherein the decellularized lung is mounted, using cannulae that are inserted into the trachea and into the pulmonary artery (Fig. S1A). Culture medium is perfused using a roller pump into the pulmonary artery. Medium from the pulmonary artery flows through the lung tissue and out the pulmonary vein, which drains into the main reservoir and thence back to the roller pump. Pulmonary artery perfusion pressures are typically 10-15/0-5 mm Hg, approximating native lung arterial pressures, with flow rates of culture medium ranging from 1-5 mL/min (Fig. S1B) (7). In order to provide negative-pressure ventilation of the engineered lung, a syringe pump is mounted to the main reservoir, which withdraws a defined volume of air to create a negative pressure within the main chamber (Fig. S1C, Fig. S2). Lung inflation under negative pressure is accompanied by inhalation of liquid medium from a trachea reservoir via a “breathing loop”. For exhalation, the syringe pump returns air to the main reservoir, forcing lung exhalation of liquid medium into the trachea reservoir. One-way valves prevent “re-breathing” of exhaled culture media on subsequent breaths. During negative pressure ventilation cycles, tracheal pressures range from 0 to -4 mm Hg (Fig. S1C).

Choice of decellularization regimen. We explored a range of conditions for lung decellularization before identifying the conditions used in these studies. Decellularization protocols were drawn from the literature and from prior experience in our laboratory (8-10). We evaluated decellularization methods based primarily on efficiency of cellular removal via routine histology. Promising conditions were further evaluated using quantitative DNA assay, mechanical testing, quantitative assays and immunostaining for specific matrix components, and imaging techniques including SEM and TEM. Solutions evaluated included various detergents (CHAPS, SDS, triton-X); deionized water; varying salt concentrations; acidic, basic and neutral pH solutions; enzymatic treatments (trypsin, DNase, benzonase); and other chemicals (including EDTA and ammonium hydroxide). Additionally, we evaluated temperature and time of exposure, and the use of vascular perfusion and airway ventilation to distribute the solution through the tissue and facilitate debris removal. The decellularization protocol described in this paper is the result of this iterated series of optimization experiments. Although still lacking in some respects, such as the removal of GAGs and fibronectin, this protocol has demonstrated promise for use in the production of a decellularized lung matrix. The decellularization process is robust, since over 300 lungs have been treated with this process and have produced similar outcomes with regard to matrix contents and architecture.

Characterization of decellularized lung scaffolds. Decellularized lung scaffolds were characterized using histological and immunofluorescent staining for collagen, elastin and glycosaminoglycans. Histological staining demonstrated preservation of collagen and elastin fibers (Fig. S4A,B), yet loss of glycosaminoglycans (Fig. S4C), consistent with quantitative assays (Fig. 2G). Additionally, immunostaining for collagen types I and IV indicated maintenance of these specific collagen molecules (Fig. S5B,C). Immunostaining for fibronectin revealed loss of fibronectin in acellular scaffolds (Fig. S5A), while laminin immunostaining indicated that laminin was retained (Fig. S5E). Although elastin was partially depleted from decellularized matrices via quantitative assay (Fig. 2G), immunostaining demonstrated retention of elastin fibers (Fig. S5D). Ultrastructural characterization of decellularized lung scaffolds is demonstrated in Fig. 2H-J, and additional images are shown in Fig. S3. These imaging studies

confirm the retention of the micro- and ultra-structural details of lung architecture, including the alveolar basement membrane and septal capillaries.

Flow cytometric analysis of isolated epithelial population. For repopulation of the epithelium of engineered lung tissues, mixed populations of neonatal rat pulmonary cells were isolated from the lungs of neonatal rat pups. Flow cytometry was used to characterize this population, and revealed the predominant cell type is type II epithelium, which are found in the alveoli and which secrete surfactant (Pro-SPC). This mixed epithelial population also includes type I epithelial cells (which line the alveoli and express aquaporin-5), Clara cells (which line distal conducting airways and bronchioles and express CCSP), and basal cells (precursor cells for columnar epithelium, which express cytokeratin-14) (Fig. S7). Additionally, the population contains mesenchymal cells (measured by α -actin expression) and endothelial cells (detected by expression of PECAM-1). A typical lung isolation contains approximately 45% type II epithelium, 2.5% type I epithelium, 5-7% Clara cells, 0.7% basal cells, as well as 5-6% mesenchymal cells and 10-20% endothelial cells. The viability of this population is over 85%, as assessed by trypan blue dye exclusion.

Optimization of reseeding techniques. Cell seeding techniques were optimized based on histological assessments of cell distribution and survival after seeding. Techniques were initially screened by assessing cell distribution after seeding, while promising techniques were further evaluated after 4-8 days of culture via histological assessment of cell morphology, proliferation, and apoptosis. Endothelial seeding methods that were evaluated included the use of bolus versus perfusion seeding, the rate of perfusion seeding, the use of a static period of varying length after seeding to enable cell adherence, and the addition of ventilation during seeding to facilitate cell distribution. Epithelial seeding techniques included the use of single or repeated bolus versus injection seeding, the rate of injection seeding, the use of a static period of varying length after seeding to enable cell adherence, and the time and rate at which perfusion and ventilation were begun after seeding. The current methods of cell seeding provide acceptable levels of coverage of the alveolar and capillary networks.

Impact of bioreactor conditions on engineered tissues.

We investigated the impact of several bioreactor variables on epithelial and endothelial attachment, growth and differentiation. Not surprisingly, we found that perfusion through the vasculature (at 2-3 mL/min), as opposed to no vascular flow, greatly enhances endothelial adhesion and survival on the lung matrix (Fig. S9A-B). We observed that negative pressure ventilation has multiple beneficial effects on cultured lung epithelium, as compared to no ventilatory movements. Intermittent ventilation of engineered lung tissues at 1 breath/min results in improves the appearance and survival of epithelium in distal alveoli (Fig. S9C-D). Additionally, ventilation helps to clear epithelial secretions from the airway tree; in the absence of ventilatory movements, the repopulated airway structures fill with cellular secretions, which stain positively for Clara cell secretory protein (CCSP, Fig. S9E-F). Clearance of airway secretions by ventilation indicates that the developing epithelium is in communication with the airway tree, and is not growing randomly within the matrix. Ventilation with air, as opposed to with culture medium, increases the numbers of type I alveolar epithelial cells, as well as the numbers of ciliated columnar epithelial cells, in the engineered lung (Fig. S9G-J). Overall, it is apparent that perfusion of the vasculature enhances endothelial survival within the matrix, while

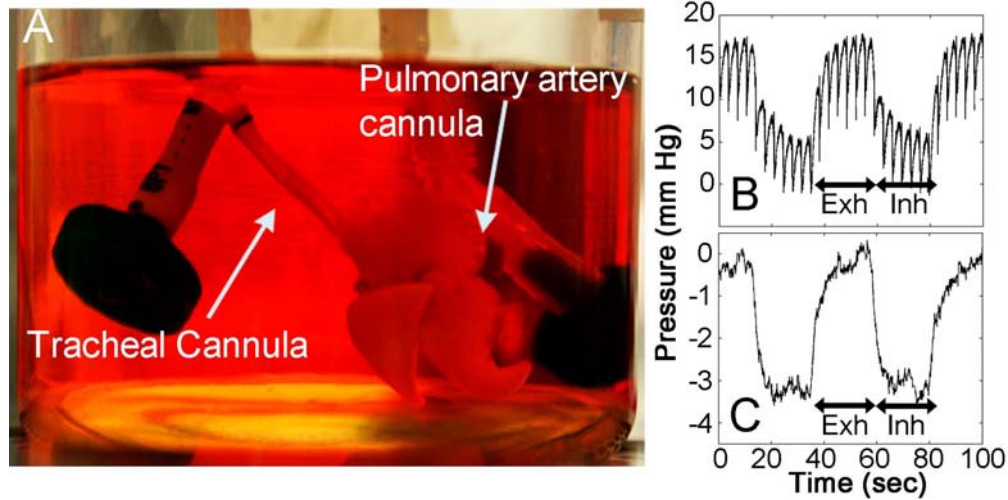
negative pressure ventilation enhances epithelial cell survival, differentiation, and airway clearance.

Engineered lungs that were cultured with negative pressure ventilation also produce pro-surfactant protein C (pro-SPC, produced by type II epithelial cells) similar to that observed in native lung (with equal protein loading as assessed by β -actin, Fig. 3E). Pro-SPC is a precursor to mature surfactant, which is important for reducing alveolar surface tension, thereby allowing lung inflation at physiologically normal pressures (11). We note that although engineered lungs contain similar levels of pro-surfactant to native lungs (Fig. 3E), it is clear from functional studies that the amount of processed, functional surfactant was less in the engineered lungs because the ‘opening pressure’ of the engineered lung is higher than for native lung, as demonstrated by the shallower slope on the compliance curve for engineered lung (Fig. 3F-H)

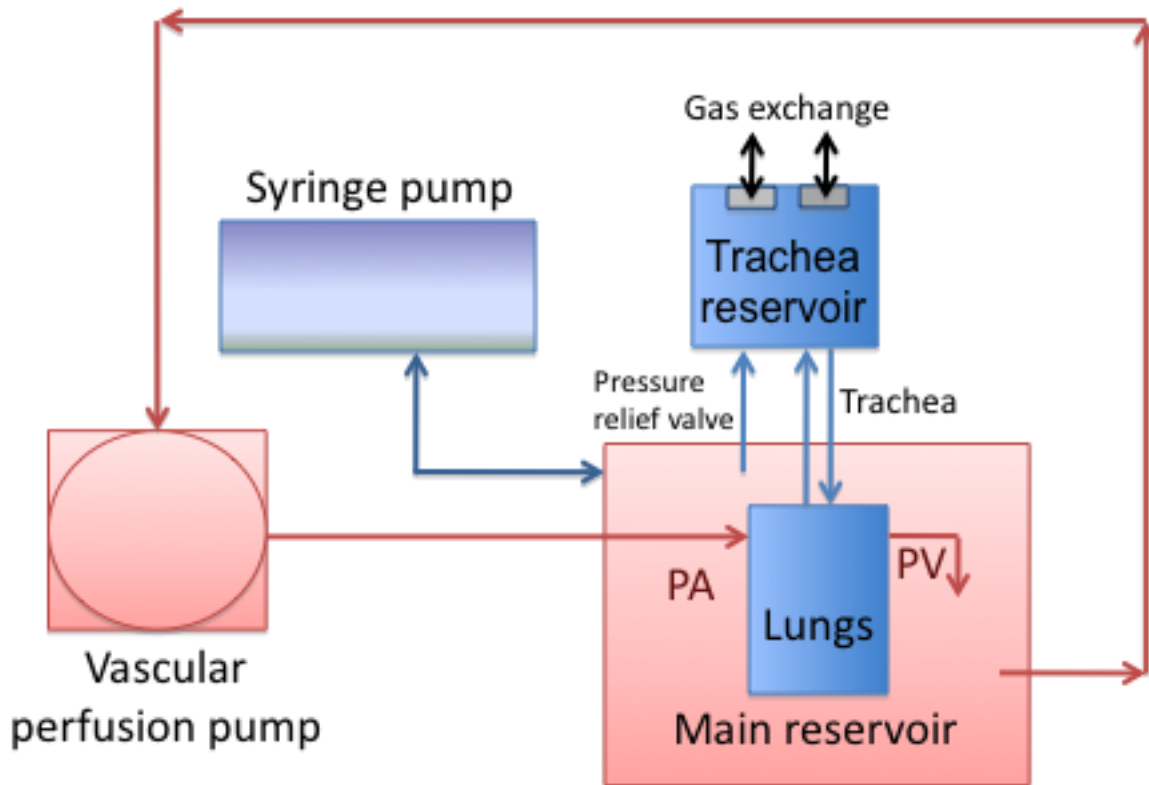
Cell populations in engineered lungs.

In addition to endothelial and epithelial cells, mesenchymal cells and epithelial progenitor cells are found in engineered lungs. Mesenchymal cells of the lung, which are involved in maintenance of the extracellular matrix, can express α actin. In native lung, these cells are diffusely distributed (Fig. S8E, α actin stained green), and are similarly distributed at both 4- and 8-days of culture in engineered lung. The presence of mesenchymal cells may contribute to maintenance of collagen matrix, and may underlie some of the retained ultimate tensile properties of engineered lungs. Additionally, progenitor cells for proximal airway epithelium are noted in engineered lungs. Cytokeratin-14 (Cy-14 in Fig. S8F) is a marker for basal cells, which are precursors for ciliated columnar epithelium of the large airways. These cells are found in larger airways in native lungs, and in multiple airway structures in engineered lung. However, engineered specimens with liquid breathing display essentially no ciliated columnar epithelium, while air breathing stimulates the growth of sparse ciliated cells in engineered large airways (Fig. S9I-J).

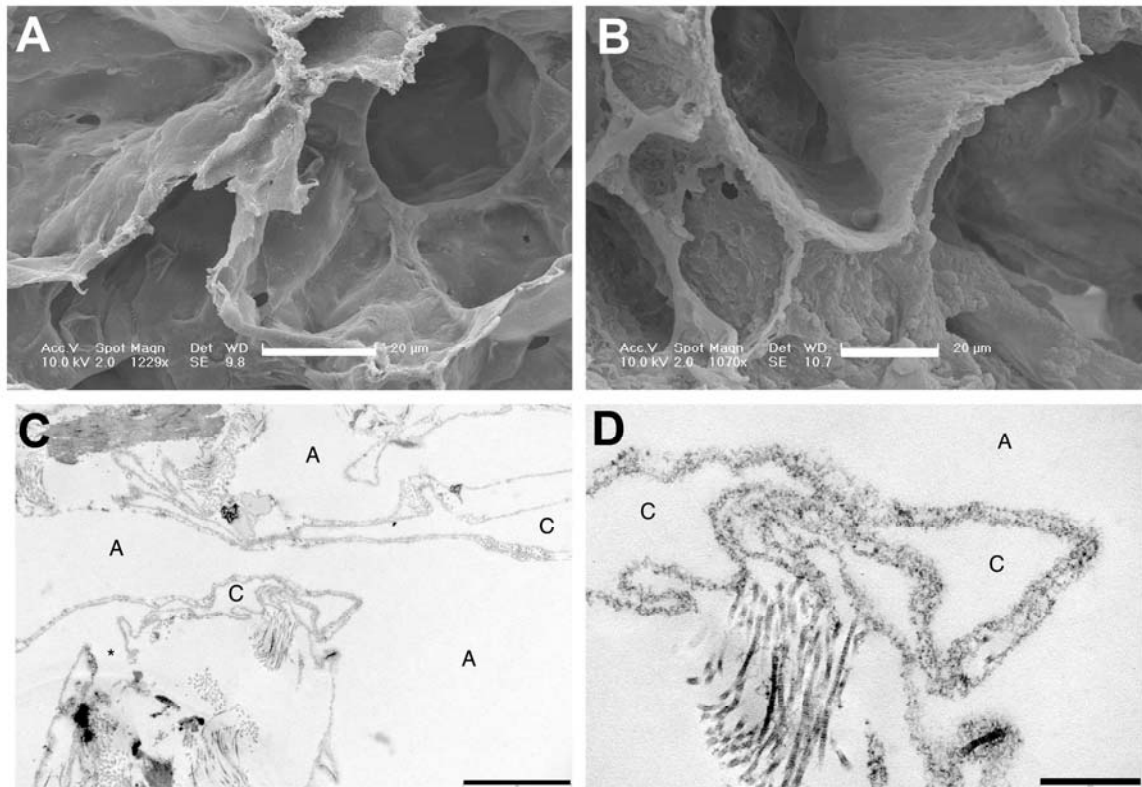
SUPPLEMENTAL FIGURES:



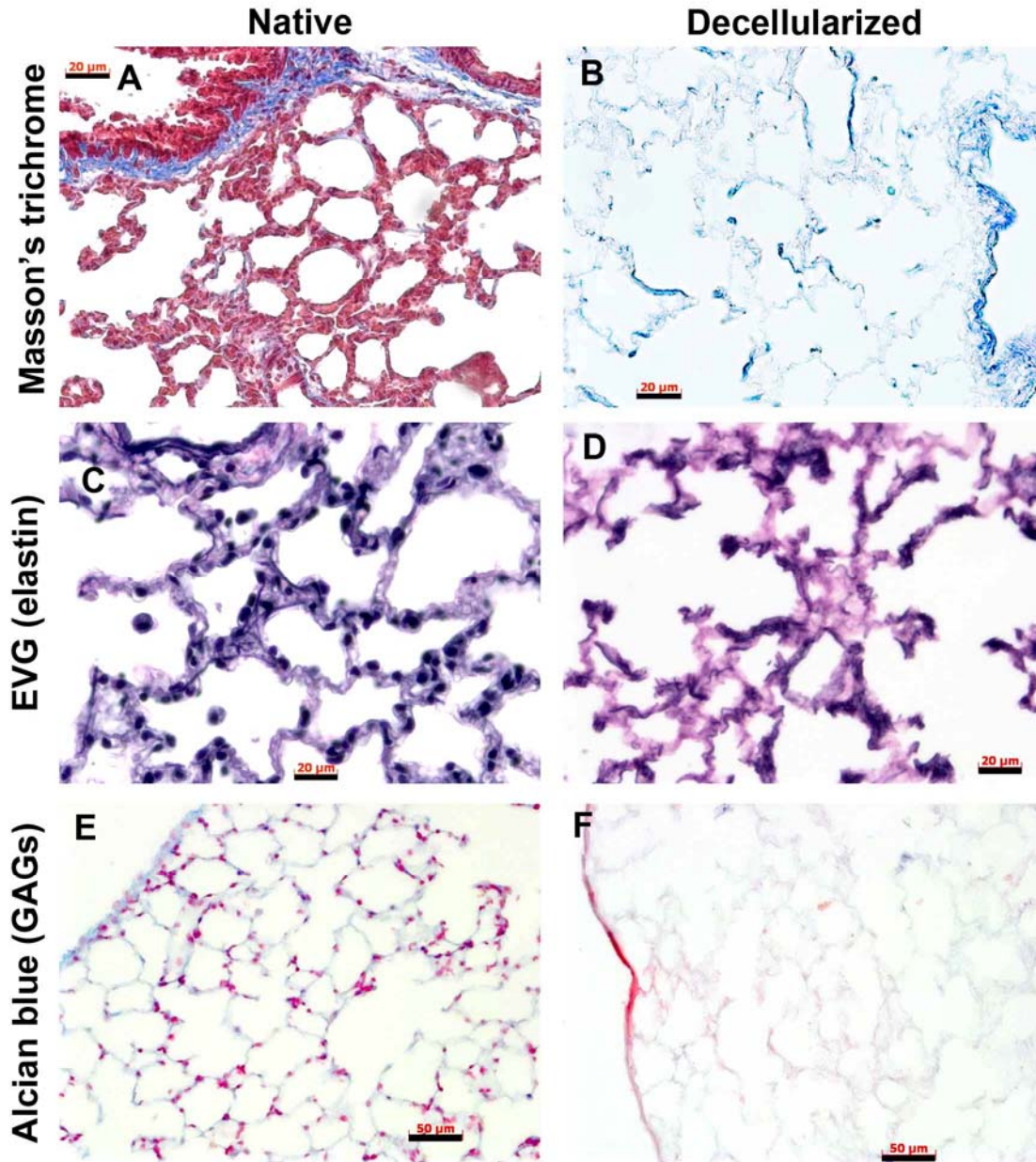
Supp Fig. 1: Lung bioreactor. A: Photo of acellular matrix suspended in main reservoir of lung bioreactor, cannulae are indicated. B: Pressure in pulmonary artery under conditions of pulsatile perfusion (high frequency oscillations) with superimposed negative pressure deflections caused by negative pressure breathing (low frequency oscillations). “Exh” is exhalation, “Inh” is inhalation. C: Pressure at tracheal inlet, showing negative pressure deflections from 0 to -4 mm Hg under action of syringe pump.



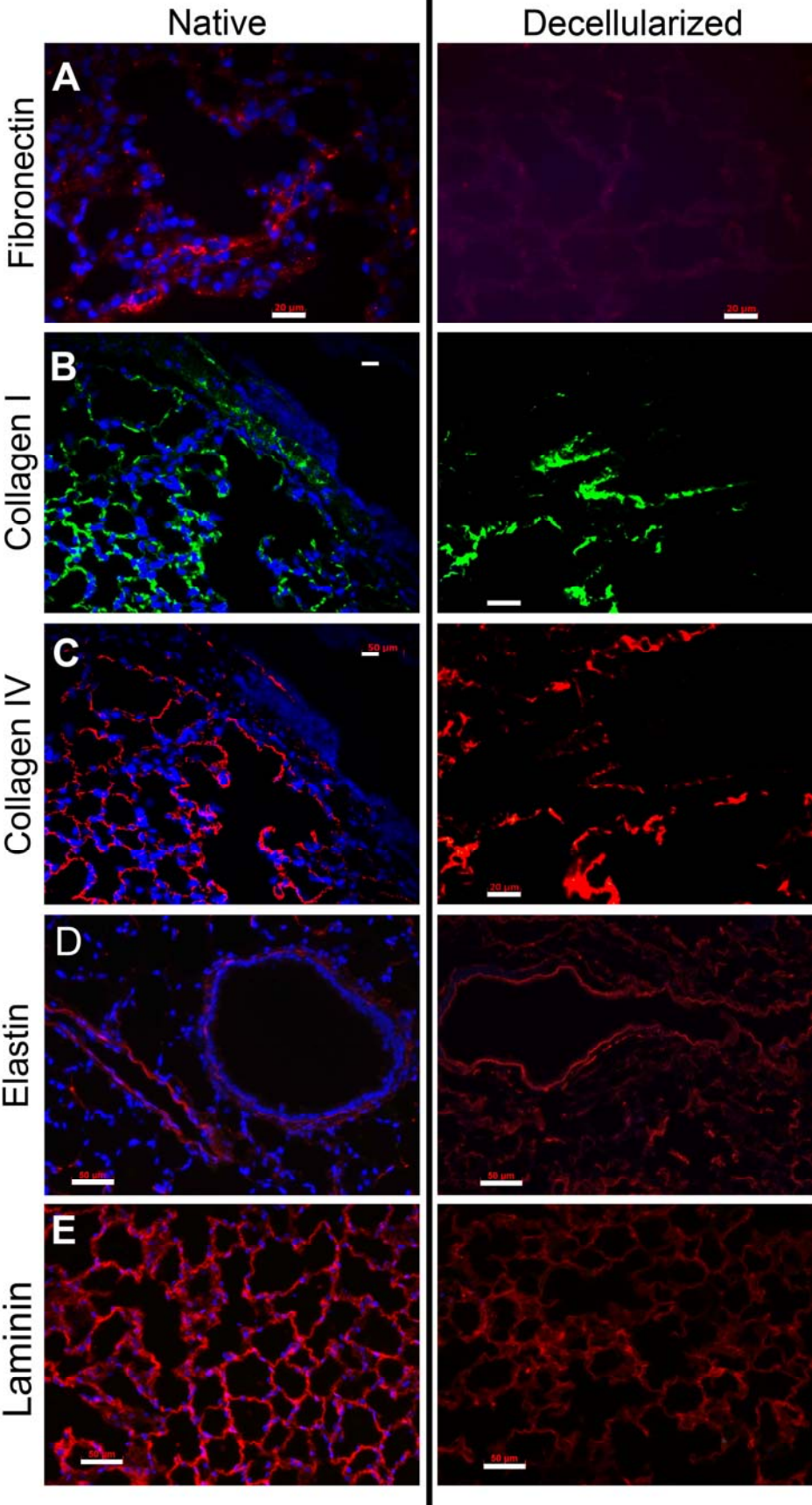
Supp. Fig. 2: Lung bioreactor schematic diagram. Schematic diagram of the lung bioreactor that provides negative pressure ventilation, perfusion pump for arterial circulation, and gas exchange occurring via the trachea reservoir.



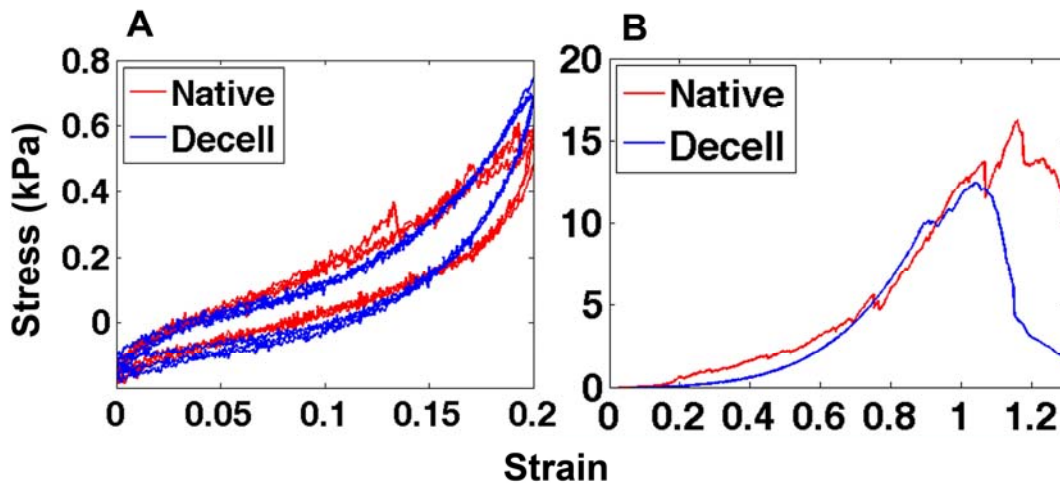
Supp Fig. 3: Ultrastructural characterization of decellularized scaffolds. Decellularized scaffolds were characterized using scanning and transmission EM. A: SEM of native lung; B: SEM of decellularized lung. Scale bars in panels A and B are 20 μm. C: TEM of decellularized lung, scale bar is 2 μm; D: TEM of decellularized lung, scale bar is 500 nm. In panels C-D, 'A' indicates alveoli, while 'C' indicates capillaries.



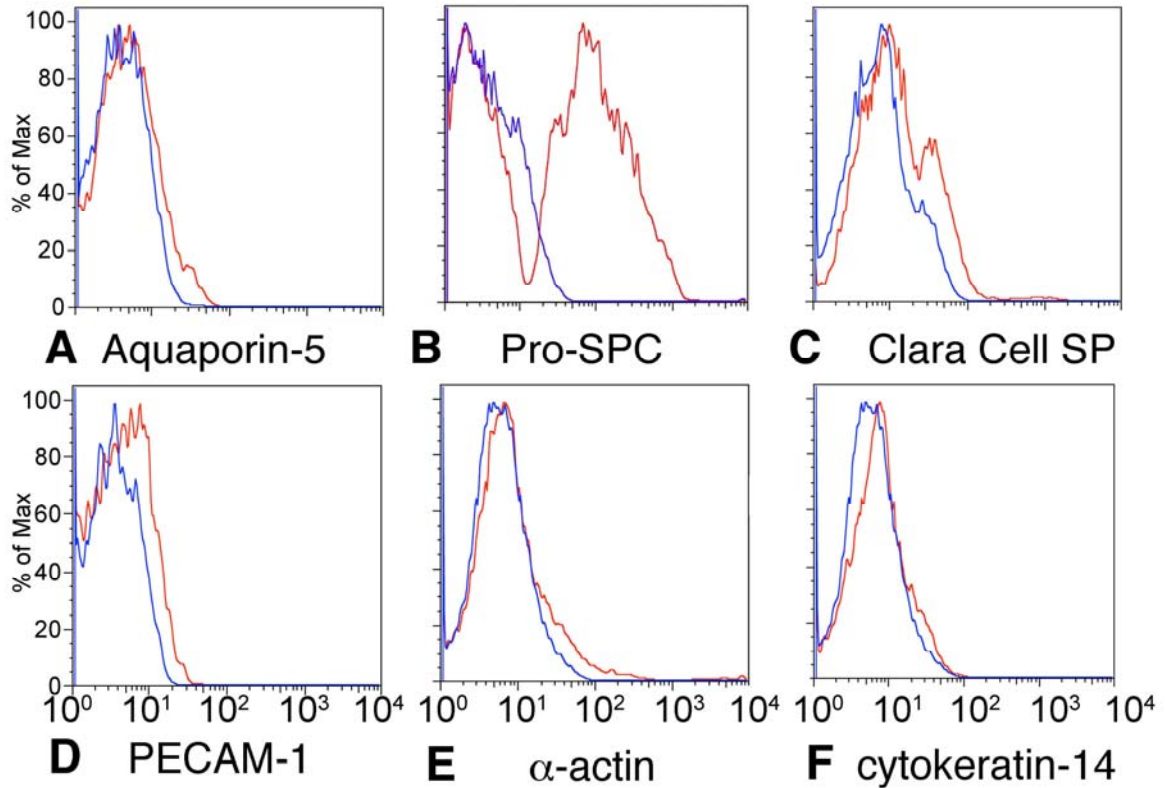
Supp Fig. 4: Histological staining of extracellular matrix markers in decellularized scaffolds. Histochemical staining of native and decellularized lung. A, B: Masson's trichrome stains collagen fibers blue; C, D: EVG staining indicates elastin fibers in black; E, F: Alcian blue stains glycosaminoglycans in blue. Scale bars are 20 μ m in panels A-D and 50 μ m in panels E-F. Staining confirms that collagen is largely preserved in decellularized tissue while nuclei (red material) are removed. In addition, there is some evidence of elastin fiber damage due to decellularization on EVG stain, which is consistent with assay findings. Lastly, depletion of glycosaminoglycans in the decellularized matrix is apparent from Alcian blue staining.



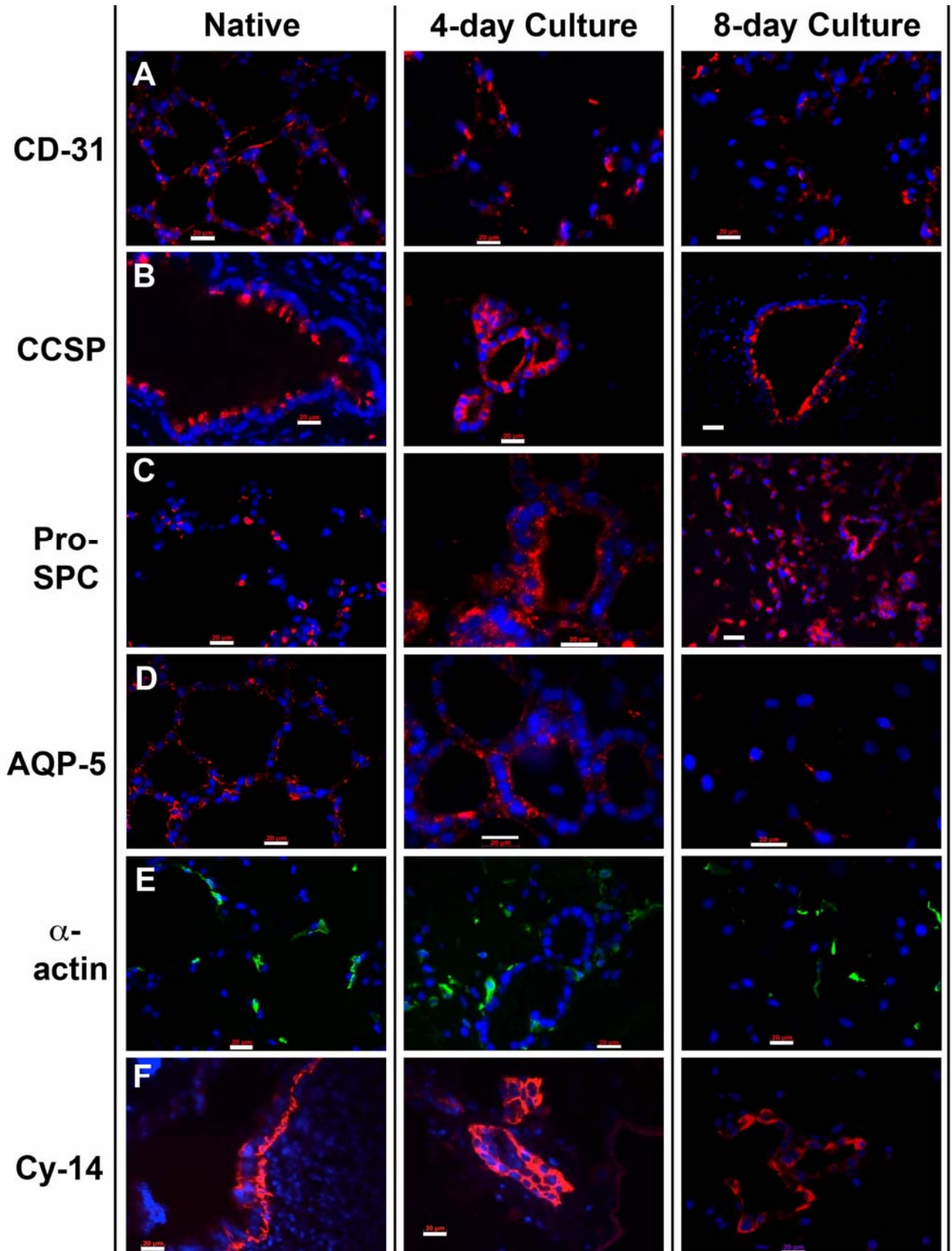
Supp Fig. 5: Immunofluorescence staining of extracellular matrix proteins in decellularized scaffolds. Native rat lung is shown in comparison with decellularized lung. Row A: Fibronectin; Row B: collagen type I; Row C: collagen type IV; Row D: elastin. Row E: laminin. In all panels, cell nuclei stain blue with DAPI, while immunofluorescent staining for specific markers appears either red or green. Scale bars are 20 μ m in Rows A-C and 50 μ m in Rows D-E.



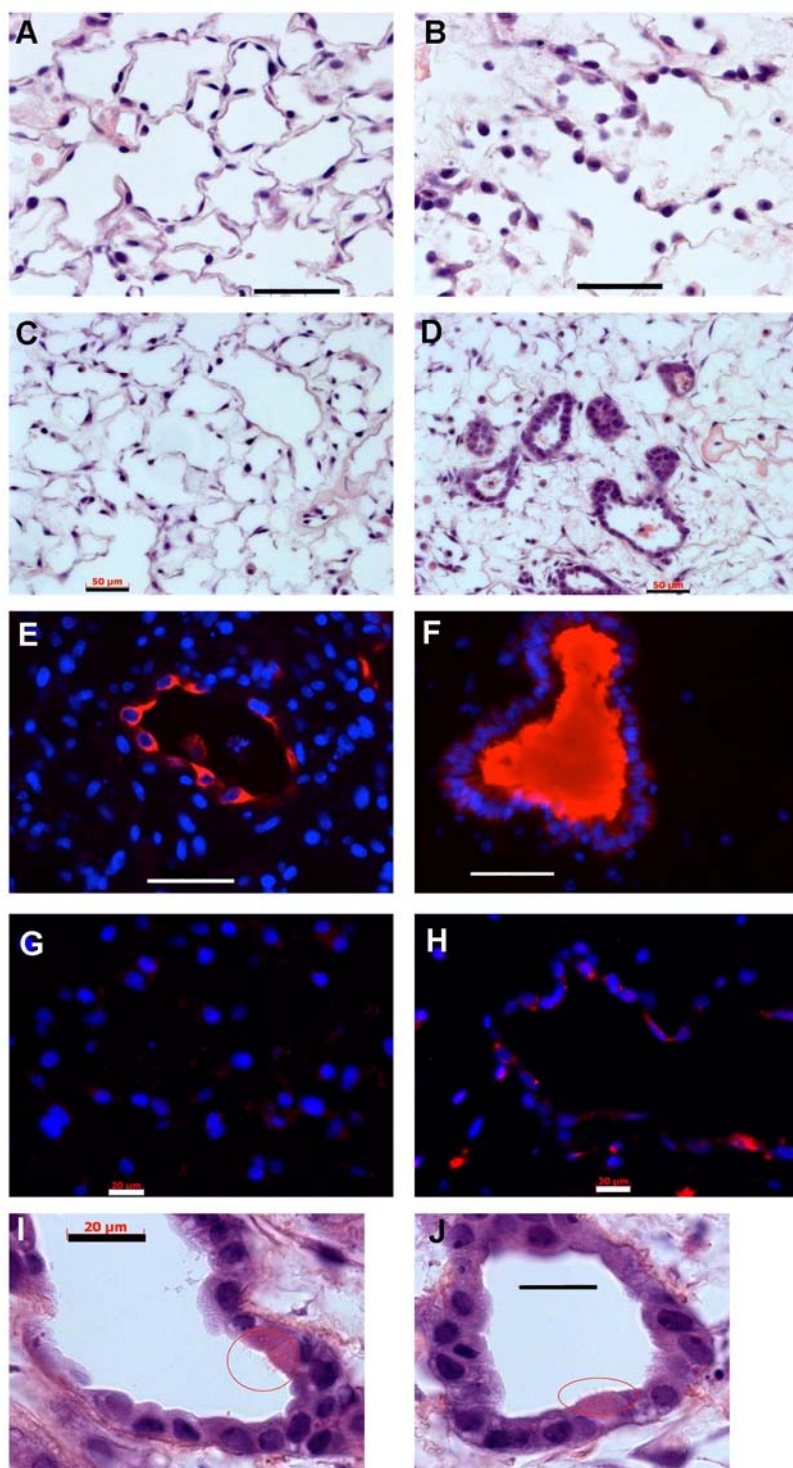
Supp. Fig. 6: Mechanical characterization of native and acellular lungs. Native and decellularized ('decell') lungs were mechanically tested. A: Stress-strain curves for native and decellularized ('decell') lungs. The elastic region is shown, demonstrating elastic recoil, hysteresis, and the absence of creep. B: Tensile strength testing for native and decellularized ('decell') lung shows similar maximal strains and stresses.



Supp Fig. 7: FACS data from neonatal rat lung isolation. A: Aquaporin-5, a specific marker for type I alveolar epithelium; B: Pro-Surfactant protein C (Pro-SPC), a marker for type II alveolar epithelium; C: Clara cell secretory protein (CCSP), a specific marker for clara cells; D: Platelet endothelial cell adhesion molecule-1 (PECAM-1, or CD-31), a marker for endothelium; E: α -actin, a marker for smooth muscle and lung mesenchymal cells; F: cytokeratin-14, a marker for basal cells. In all panels, isotype control is in blue, antibody stain is in red.

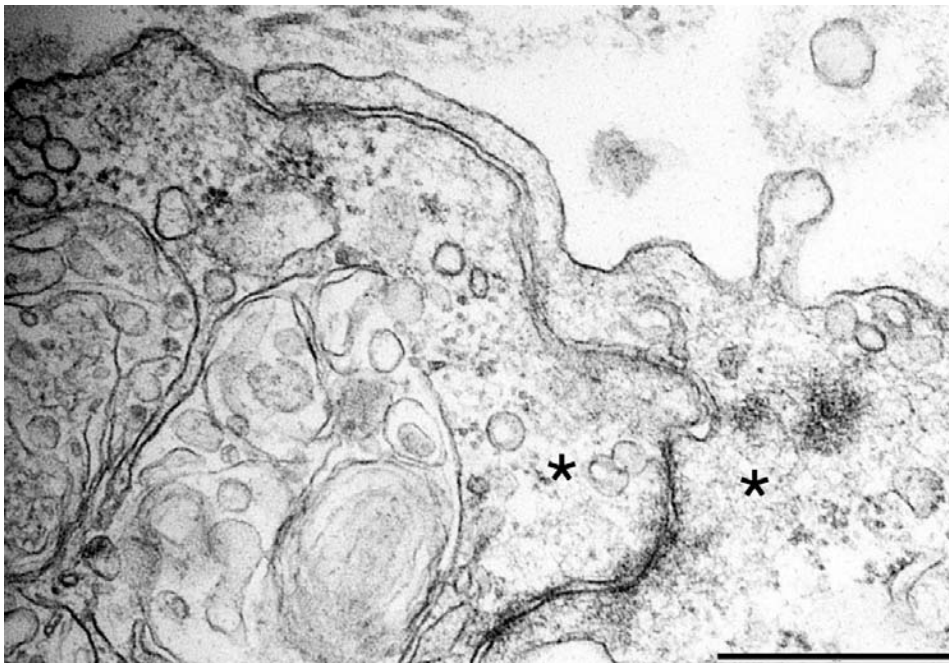


Supp Fig. 8: Cell populations in engineered lung. Native rat lung is shown in comparison with engineered lungs that are cultured for either 4 or 8 days. Row A: Endothelial cells stained with CD-31; Row B: CCSP, a marker for Clara cells; Row C: Pro-SPC, a marker for type II alveolar epithelial cells; Row D: AQP-5, (aquaporin-5), a marker for type I alveolar epithelial cells; Row E: α actin, a marker for vascular smooth muscle and lung mesenchymal cells; Row F: Cy-14 (cytokeratin-14) a marker for basal cells which are precursors for columnar epithelium. In all panels, cell nuclei stain blue with DAPI, while fluorescent immunohistochemical staining for specific markers appears either red or green. Scale bars are 20 μ m in all panels

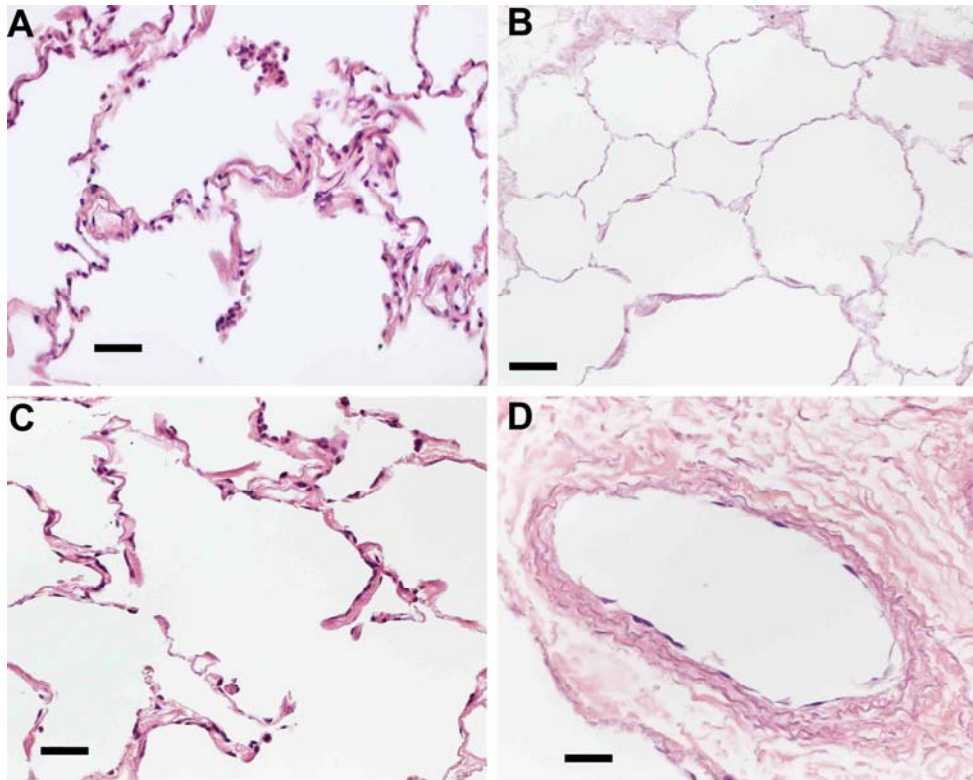


Supp Fig 9: Impact of bioreactor conditions on lung cell culture. A: H&E stain of rat lung microvascular endothelial cells cultured on acellular matrix with vascular flow of 3 mL/min for 8

days, cells are adherent and spread on the matrix; B: H&E stain of endothelial cells cultured for 8 days without vascular flow, cells are rounded and poorly attached. C: H&E stain of rat lung epithelial cells cultured for 8 days with negative pressure breathing at 1 breath per minute; D: epithelial cells cultured without negative pressure breathing, showing formation of multiple airway-like structures lined with cuboidal cells. E: Immunofluorescence for CCSP (red), with nuclei stained blue with DAPI, showing airway lumen lined by epithelial cells expressing CCSP when cultured under conditions of negative pressure breathing; F: CCSP protein accumulates in airways in lungs that are not breathed during culture. Scale bars in panels A-F are 50 μm ; G: Aquaporin-5 stain in 8-day cultures with liquid breathing; H: Aquaporin-5 in 8-day cultures with air breathing shows increased expression. Panels E-H, nuclei stain blue, antigen stains red. I, J: H&E stain of 8-day cultures with air breathing, red circles show cilia. Scale bars in panels G-J = 20 μm .



Supp Fig. 10: Tight junction formation in engineered endothelium. Endothelial cells cultured in engineered lung tissue for 8 days demonstrate formation of tight junctions via TEM. Asterisks indicate adjacent endothelial cells. Scale bar is 500nm.



Supp Fig. 11: Decellularization and repopulation of human lung. A: Native human lung shows alveolar structures; B: after 6 hours of decellularization; C: repopulation of acellular human lung matrix with A549 epithelial cell line; D: repopulation with human endothelial cells. All panels are H&E stain, scale bars are 50 μm

Tables:

Table S1

Antibody	Source	Antibody Concentration	
		Western Blot	Immunofluorescence
α -actin	Abcam	n/a	1:1000
β -actin	Sigma	1:2000	n/a
Aquaporin-5	Millipore	n/a	1:1000
Clara Cell Secretory Protein	Barry Stripp (Duke)	n/a	1:20,000
Collagen I	Abcam	n/a	1:200
Collagen IV	Abcam	n/a	1:500
Cytokeratin-14	Thermo Scientific	n/a	1:100
Elastin	Abcam	n/a	1:100
Fibronectin	Abcam	n/a	1:100
Laminin	Abcam	n/a	0.02 mg/mL
MHC Class I	Abcam	1:1000	n/a
MHC Class II	Abcam	1:1000	n/a
PECAM-1	Santa Cruz	n/a	1:100
Pro-Surfactant Prot C	Millipore	1:500	1:1000
Surfactant Prot B	Santa Cruz	1:200	n/a

Supplemental References:

1. S.L.M. Dahl, J. Koh, V. Prabhakar, L.E. Niklason, *Cell Transplant.* **12**, 659 (2003).
2. L. Gui, S. Chan, C. Breuer, L. Niklason, *Tissue Eng. C* **16**, 173 (2010).
3. A.C. Kiser, P. Ciriaco, S.C. Hoffmann, T.M. Egan, *J. Thor. Cardiovasc. Surg.* **122**, 18 (2001).
4. R.A. Grant, *J. Clin. Path.* **17**, 685 (1964).
5. R. Foronjy *et al.*, *Am. J. Physiol. Lung Cell. Mol. Physiol.* **294**, L1149 (2008).
6. J. Melero-Martin *et al.*, *Blood* **109**, 4761 (2007).
7. P.E. Sharp, M.C. LaRegina, *The Laboratory Rat* (CRC Press, 1998).
8. A. Bader *et al.*, *Eur. J. Cardiothor. Surg.* **14**, 279 (1998)
9. T.W. Gilbert, T.L. Sellaro, S.F. Badylak, *Biomaterials* **27**, 3675 (2006).
10. Y.M. Lin, A.R. Boccaccini, J.M. Polak, A.E. Bishop, V. Maquet, *J. Biomat. Appl.* **21**, 109 (2006).
11. L.G. Dobbs, *Ann. Rev. Med.* **40**, 431 (1989).